Chemical Engineering Journal 482 (2024) 148894

Contents lists available at ScienceDirect

Chemical Engineering Journal

journal homepage: www.elsevier.com/locate/cej

Safety parameters and stability diagram of hydroxylamine hydrochloride and sulphate

Giuseppe Andriani [a], Gianmaria Pio [b], Chiara Vianello [a], Paolo Mocellin [a,*], Ernesto Salzano [b]

[a] Università degli Studi di Padova, Dipartimento di Ingegneria Industriale, Via Marzolo 9, 35131 Padova, Italia
[b] Università di Bologna, Dipartimento di Ingegneria Civile, Chimica, Ambientale e dei Materiali, Via Terracini 28, 40131 Bologna, Italia

ARTICLE INFO

Keywords:
Thermal decomposition
Stability diagram
Storage safety
Hydroxylamine
Salts

ABSTRACT

The thermal instability of hydroxylamine (HA) poses severe concerns in the process industry, while preventive and mitigative strategies are required to reduce the frequency and magnitude of associated decomposition phenomena. From this perspective, formulating an aqueous solution or using derived salts could be a solution for risk reduction. Nevertheless, the effect of HA-derived salt addition on HA/water solutions has yet to be reported in the literature. For this reason, the scope of the present work is to examine experimentally whether salt addition can reduce the occurrence and severity of HA thermal degradation. Samples containing HA and hydroxylamine sulphate (HAS) or hydroxylamine hydrochloride (HH) were analysed. During the experimental campaign, a calorimeter was used for the assessment of reaction kinetic, thermodynamic, and onset features. The determined parameters were used for safety purposes to understand the related thermal hazards and to provide stability diagrams. The results show, under certain conditions, that the type and amount of HA-derived salt determines an attenuation of the decomposition of HA/water solutions. Moreover, increasing the amount of salt enhances the susceptibility to decomposition of the HA/water solution, while lower salts content could help stabilise the HA mixtures. According to the developed stability diagram, an inherently safe zone for reaction or storage has been established. Eventually, the proposed structured approach can be intended as a strategic procedure to involve the reaction parameters gathered, which is helpful for drawing general guidelines for establishing safer processes and reaction conditions.

1. Introduction

Hydroxylamine (HA) is a well-known molecule involved in several chemical [1] and biochemical [2,3] reactions. From an industrial perspective, more than 95 % of hydroxylamine production is currently used to synthesise cyclohexanone oxime or caprolactam [4]. Otherwise, HA can be involved as a flaking-off and a metallic surface treatment agent in the semiconductor and pharmaceutical industries, as well as an essential feedstock for dyes, rust inhibitors, and products such as painkillers, antibiotics, and tranquillisers [5]. It is well-established that HA is prone to violent decomposition reactions leading to runaway conditions when processed in chemical equipment or contained in storage vessels. Indeed, mixtures with elevated HA purity start to decompose at almost ambient temperature [6]. For concentration in water greater than 70 % w, detonation features are associated with decomposition [7]. For this reason, HA is present on the market as an aqueous solution with a maximum concentration of 50 %w [8] or as a part of derived salts [9]. Despite these handling precautions, HA was involved in two significant accidents in the USA and Japan [10], characterized by similar conditions. In both cases, a distillation process unit was processing HA solution with a concentration greater than 80 %w, resulting in detonation features because of overheating [11,12]. Although the instability of mixtures containing HA poses deep concerns regarding the safety of industrial plants, recent trends in industrial fields also recorded an increased interest in HA-salt solutions [9]. Among the others, hydroxylamine hydrochloride (HH), hydroxylamine sulphate (HAS), hydroxylamine nitrate (HN), and hydroxylamine phosphate (HP) are worth to be mentioned. Hence, it is worth noting that some HA-salts accidents are also reported within the ARIA database [13]. Even if the scenarios are only provided in qualitative terms, and quantitative information is not registered, explosions occurred in the pharmaceutical and nuclear industries. Additional accidents involving hydroxylamine nitrate (HN) are reported respectively in the FACTS database [14] in a waste treatment plant and a road transport facility.

A fundamental-oriented characterisation of the most relevant phe-

* Corresponding author.
E-mail address: paolo.mocellin@unipd.it (P. Mocellin).

https://doi.org/10.1016/j.cej.2024.148894

Available online 21 January 2024

Nomenclature

Symbols

ARC	Accelerating Rate Calorimetry
B	Dimensionless heat of reaction
B_{crit}	Critical value of the dimensionless heat of reaction
C_{A0}	Initial molar concentration of the main reactant A
$\widehat{C}_p$	Heat capacity per unit mass of the reactive mixture
$\widetilde{C}_p$	Heat capacity per unit moles of the reactive mixture
$\widetilde{C}_p^0$	Heat capacity per unit moles in the standard state
$\overline{\widetilde{C}_p^0}$	Partial molar heat capacity in the standard state
$\widehat{C}_{p,cell(T)}$	Heat capacity per unit mass of the cell as a function of temperature
$\widetilde{C}_{p,s(T)}$	Heat capacity per unit moles of the electrolytic solution as a function of temperature
$\widehat{C}_{p,sample(T)}$	Heat capacity per unit mass of the sample as a function of temperature
$\widetilde{C}_{p,sample(T)}$	Heat capacity per unit moles of the sample as a function of temperature
$\widetilde{C}_{p,sample}\Big\vert_{T_{max}}$	Heat capacity per unit moles of the sample at the maximum temperature
$\widetilde{C}_{p,sample}\Big\vert_{T_{onset}}$	Heat capacity per unit moles of the sample at the onset temperature
CSTR	Continuous stirred tank reactor
Da	Damköhler number
$\left(\frac{dT}{dt}\right)_{baseline}$	Ramped temperature rise rate set at the beginning of the experiment
$\left(\frac{dT}{dt}\right)_{measured}$	Measured temperature rise rate starting from the onset time
DSC	Differential Scanning Calorimetry
E_a	Apparent activation energy
HA	Hydroxylamine
HAS	Hydroxylamine sulphate
HH	Hydroxylamine hydrochloride
HN	Hydroxylamine nitrate
HP	Hydroxylamine phosphate
hr	Heating rate
k_k	Apparent kinetic constant
$k_k\vert_{T_0}$	Apparent kinetic constant evaluated at the initial temperature
$k_{k\infty}$	Apparent Arrhenius pre-exponential factor
m_{cell}	Mass of the cell
m_{sample}	Mass of the sample contained in the cell
n	Apparent reaction order
P	Pressure
PFR	Plug flow reactor
QRA	Quantitative risk analysis
R_g	Universal gas constant
$S(\theta^*;B)$	Normalized objective sensitivity
$s(\theta^*;B)$	Objective sensitivity
T	Temperature
T_0	Initial temperature
TGA	Thermogravimetric Analysis
TMR_{ad}	Time to maximum rate under adiabatic conditions
TS^U	Thermal Screening Unit
t	Time
t_B	Batch time
VMWT	Varma, Morbidelli and Wu's theory
x	Molar fraction

Subscript

1	Subscript denoting the thermodynamic state before dissolution
2	Subscript denoting the thermodynamic state after dissolution
i	Subscript denoting a reference salt
j	Subscript denoting a particular ion
max	Subscript denoting conditions related to the exothermic peak
$onset$	Subscript denoting onset conditions
$solvent$	Subscript denoting the solvent of an electrolytic solution

Greek symbols

γ	Dimensionless activation energy
$\gamma^{\pm}$	Mean activity coefficient
$\Delta\widetilde{H}_d$	Enthalpy of the decomposition reaction at the mean value between onset and decomposition temperature
$\Delta\widetilde{H}_{f,i}$	Formation enthalpies for reagents and products
$\Delta\widetilde{H}_r$	Molar enthalpy of reaction
$\Delta\widetilde{H}_{vap}$	Molar heat of vaporization of water at the mean value between onset and decomposition temperature
ΔT_{ad}	Adiabatic temperature rise during the reaction
θ	Dimensionless temperature
θ^*	Dimensionless temperature maximum
ρ	Density of the reactive mixture
$\Phi_{(T)}$	Correction factor to account for the non-perfect adiabaticity as a function of temperature
χ	Conversion of the main reactant

nomena is highly desirable to identify the critical conditions and mitigate possible consequences of these scenarios. Although the relevance of the subject, a poor understanding of the chemical interactions between HA and salts can be observed in the literature. Indeed, to the best of our knowledge, studies need to be provided in the literature investigating the influence of HA-derived salts on the thermal decomposition of HA aqueous solutions. In this perspective, the current knowledge of HA decomposition is reported at first. Previous investigations available in the current literature [15,16] have pointed out that the mechanism ruling the thermal decompositions of HA/water solution depends on pH. More specifically, it has been hypothesised that in an acid environment, the apparent chemical reaction reported in Eq. (1) prevails, whereas, in a basic solution, Eq. (2) dominates.

$$4NH_2OH \rightarrow N_2O + 2NH_3 + 3H_2O \quad (1)$$

$$3NH_2OH \rightarrow N_2 + NH_3 + 3H_2O \quad (2)$$

This is particularly relevant since HA in water acts as a base, and a water solution of HA 50 %w has a pH of 10.6. However, the hypothesized mechanism is in contrast with the enthalpy of the reaction ($\Delta\widetilde{H}_r$) calculated by Cisneros et al. [17], showing an endothermic behaviour. Hence, Eq. (2) cannot be representative of the exothermic behaviour observed during the thermal decomposition. Subsequently, a possible alternative apparent chemical reaction has been proposed [18] based on the measured composition of the gaseous species obtained after decomposition, as reported in Eq. (3).

$$157NH_2OH_{(l)} \rightarrow 61NH_{3(g)} + 35N_{2(g)} + 12N_2O_{(g)} + 2NO_{(g)} + 143H_2O_{(g)} + H_{2(g)} \quad (3)$$

In this case, the $\Delta\widetilde{H}_r$ calculated by Cisneros et al. (2003) is similar to the values measured in the same work as well as the one experimentally collected in a more recent investigation [19], confirming the reliability of Eq. (3) to reproduce the observed nature of the degradation phenomenon involving HA from a thermodynamic perspective.

Regarding HA-derived salts, the main analysed compounds are hydroxylamine hydrochloride (HH) [20], hydroxylamine sulphate (HAS) [21], hydroxylamine nitrate (HN) [22,23], and hydroxylamine phosphate (HP) [19]. According to [24] and [16], the apparent overall decomposition reactions of HH and HAS can be expressed as reported in Eq. (4) and Eq. (5), respectively. In contrast, the formation of ammonium sulphate for HAS and nitric acid for HN has been proposed by [19], following the reactions reported in Eq. (6) and Eq. (7). Hence, the formation of ammonium chloride from the decomposition of HH can also be presumed, even if Gigante et al. (2004) have not proposed an apparent chemical reaction. However, it is worth noting that water solutions of HA-derived salts exhibit exothermic decomposition reactions less violent than those involving HA/water solutions [19].

$$255.25NH_2OHHCl_{(l)} \rightarrow 107.75NH_{3(g)} + 8.5N_2O_{(g)} + 212.25H_2O_{(g)} + 255.25HCl_{(g)} + 64.8N_{2(g)} + 16.8O_{2(g)} + 0.9NO_{(g)} + 9H_{2(g)} \quad (4)$$

$$2(NH_3OH)_2SO_{4(s)} \rightarrow 2SO_{3(g)} + N_2O_{(g)} + 2NH_{3(g)} + 5H_2O_{(g)} \quad (5)$$

$$3(NH_3OH)_2SO_{4(s)} \rightarrow (NH_4)_2SO_{4(s)} + 2SO_{2(g)} + 2N_2O_{(s)} + 8H_2O_{(s)} \quad (6)$$

$$3NH_2OHHNO_3 \rightarrow 2HNO_3 + N_2 + N_2O + 5H_2O \quad (7)$$

Other than the chemical composition of salts, additional parameters can affect the decomposition of HA-water solutions. Indeed, further studies addressed the influence of transition metals on the decomposition of HA and their derived salts [25,26] or the effect of the material of the container used for the experiments on the decomposition [21]. Remarkably, results reveal that the presence of Cr^{3+}, Co^{2+} or Cu^{2+} ions in an aqueous solution can inhibit the decomposition reaction of HN and induce endothermic decomposition of HN instead of exothermic. In contrast, Co^{3+} ions can inhibit both HH and HN decomposition reactions. Conversely, stainless steel, carbon steel, and titanium containers can catalyse the decomposition of HA or its derived salts. Thus, to reduce the occurrence of harmful decomposition reactions, attention must be paid during process or equipment design, favouring the presence of specific types of ions in aqueous solution and avoiding designing equipment with particular materials.

Under the fluid dynamic hypothesis of a well-mixed phase, an ideal adiabatic batch reactor was modelled to represent the worst-case scenario in which the characteristic time of reaction is much lower than the characteristic time for heat exchange, thus establishing adiabatic conditions. Governing dimensionless molar and heat balance equations are reported in Eqs. (8) and (9). The definitions of the involved dimensionless model parameters *Da*, θ, γ and *B* can be retrieved in [27] being the Damköhler number equal to the dimensionless batch time and the dimensionless heat of reaction also equal to the dimensionless adiabatic temperature rise.

$$\frac{d\chi}{dDa} = \exp\left(\frac{\theta}{1+\theta/\gamma}\right)(1-\chi)^n \quad (8)$$

$$\frac{d\theta}{dDa} = B\frac{d\chi}{dDa} \quad (9)$$

According to the Varma Morbidelli Wu Theory (VMWT) [28], stability diagrams can be produced for batch reactors using dimensionless reactor maximum temperature, whereas θ^* and *B* are considered as the measurable for the sensitivity analysis. Diagrams determined using sensitivity methods based on the VMWT can be regarded as a runaway prevention methodology available during processes and equipment's design and optimization phase [29]. Typically, a stability diagram for reactive chemical systems reports a dimensionless index of reactivity against a dimensionless index of exothermicity. Depending on the selected dimensionless variables, the topological aspect of the maps could vary. In analogy with the work done in the VMWT for continuous reactors, using *Da* as an index of reactivity and *B* as an index of exothermicity, the stability diagram appears as in Fig. 1. More specifically, a monotonic decreasing curve with upward concavity delimits a runaway and a safe region [30].

However, the VMWT cannot be involved in an adiabatic batch reactor because intrinsically hazardous conditions can be permanently established for *Da* sufficiently large. Large *Da* means large *t*, which implies χ practically equals unity and temperature profiles wholly developed. Indeed, for a specific combination of the system-independent parameters (i.e., *n*, γ and *B*), the system's sensitivity becomes dependent on the *Da* number, and the generality of the criteria is lost. In other words, it can also be stated that the sensitivity analysis is based on the concept of equilibrium and stability of equilibriums. In batch or continuous systems, a thermal equilibrium can be found by balancing thermal energy generation and dissipation. This balance cannot be reached in adiabatic systems because the system can only generate and accumulate thermal energy. Thus, it can reach practically an unstable equilibrium, and the parametric sensitivity analysis cannot be applied. However, it can be pointed out that process parameters like C_{A0} and T_0 are crucial for preventing runaway conditions and reducing the severity of thermal phenomena. Hence, despite all, a methodology for quantifying C_{A0}, T_0 and *t* able to prevent and limit undesired thermal phenomena is required.

For this reason, the present work presents a modified version of runaway-based criteria for developing systems stability diagrams using the information obtained through calorimetric analysis. The calorimetric study is a crucial experimental technique that involves measuring the heat exchanges between a sample and its surroundings associated with chemical reactions, physical processes, or phase transitions. It provides valuable insights into the thermodynamic, kinetic and safety properties of the investigated substances [31]. Different calorimetric techniques can be applied experimentally, such as DSC, TGA, isothermal calorimetry and reaction calorimetry [32]. In a DSC, the heat flow into or out of a sample as a function of temperature or time is measured [33] In contrast, in a TGA, the weight changes of a sample as a function of temperature or time are monitored while the sample is subjected to a controlled atmosphere [34]. During isothermal calorimetry, the temperature of the sample is kept constant while heat flow is measured [35]. Eventually, with a reaction calorimetry, it is also possible to study the generated heat or absorbed during a chemical reaction [36]. Two examples of reaction calorimetry are bomb calorimetry [37] and ARC [38]. In the present study, a Thermal Screening Unit (TS^U) is employed.

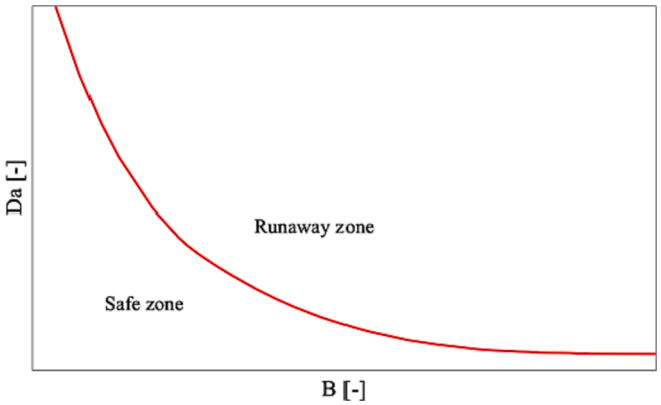

Fig. 1. Schematic representation of a Da-B stability diagram.

This is an experimental apparatus able to perform an ARC calorimetry, heating a sample at a constant rate by an oven and measuring the temperature and pressure profile as a function of time to assess thermodynamic, kinetic and safety parameters of a reacting mixture [39].

In this framework, this study focused on the decomposition kinetics of HA/water/HA-derived salt solutions using experimental measurements. In particular, the HA-derived salts studied were HH and HAS. The experiments were conducted in a TS^U, following the methodology of similar studies [40]. The obtained results were used to assess the critical conditions leading to runaway developing reactor stability diagrams, following an innovative procedure based on VMWT. More specifically, the safe-to-runaway transition curve was determined using a sensitivity-based approach as well as by determining the dimensionless reaction time (i.e., the *Da* value) at which T_{onset} and $dT/dt = 0$ are reached, to test the robustness of the obtained results.

2. Materials and methods

The methodology implemented in this work consists either of data collection or data elaboration phases. In this sense, the description of the procedure is divided into subsections. More specifically, a brief presentation of the experimental setup and sample analysis is provided in Section 2.1. The primary safety parameters considered in this work are presented (Section 2.2), and the data analysis methodology is elucidated (Section 2.3). Subsequently, a procedure to account for the obtained parameters in safety evaluations is described in Section 2.4 based on the construction of stability diagrams for the system. For the sake of clarity, the general logical workflow followed in the present work is reported in Fig. 2. It is worth mentioning that the proposed procedure is generalisable and applicable to a wide variety of compounds that exhibit thermal degradation features to quantify the hazard related to the instability of the considered compound and to support decision-making related to intrinsic and extrinsic protective actions when sizing and operating reactors and storage systems.

2.1. Experimental procedure

Samples were prepared from aqueous solutions of HA, adding HH and HAS in salt form and 99.999 %w pure, supplied by Sigma-Aldrich®. First, HA/water solutions were arranged with 50 %w, 30 %w and 10 %w of HA by dilution with demineralized water. Then, the HA/water/salt solutions were realized, adding 30 %w, 20 %w, 10 %w, 2 %w and 1 %w of HH and HAS to the different HA/water solutions, stirring till complete dissolution. %w refers to the HA/water solution. Thus, for example, a solution with 50 %w of HA and 20 %w of salt is formed by 0.5 g of water, 0.5 g of HA and 0.3 g of salt. For the sake of comparison, water solutions with only HA 50 %w, 30 %w and 10 %w were also prepared and analysed. The equipment used for the experimental campaign is the TS^U made by HEL Group Ltd, described by Vianello et al. (2018) [41], and a schematic representation of the equipment has been reported in Fig. 3. For the screening tests, two constant oven heating rates (hr) were chosen respectively equal to 2 and 5 °C min^{-1}. The cell used for all tests is made

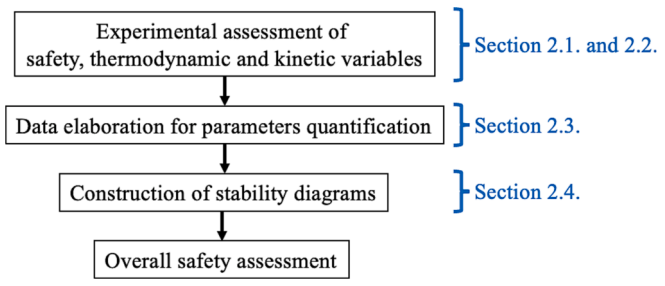

Fig. 2. The logical workflow implemented in this work for the characterization of safety aspects.

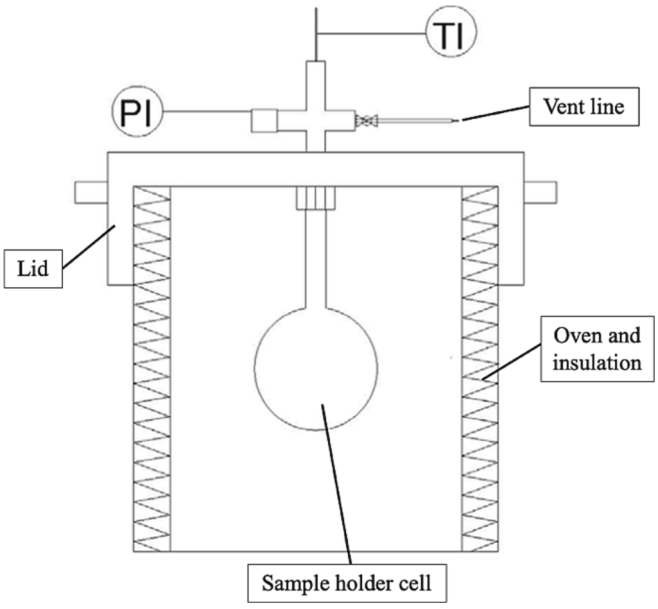

Fig. 3. Schematic representation of the TS^U.

by Hastelloy C276 to guarantee a negligible influence of the material of the container on the collected data as well as elevated resistance to the highly corrosive environment. The sample temperature was measured by a type K calibrated thermocouple, and the internal cell pressure was monitored using an Omega Engineering 1–200 bar pressure gauge with a reliability of 0.2 bar. WinISO® is the software used to control hardware and acquire temperature and pressure data from the TS^U. Unless otherwise stated, measurements were performed in line with the following experimental procedure: sample preparation, cell filling, hermetic sealing of the sample cell onto the TS^U, seal checking, heating ramp, cooling to ambient temperature, and vessel venting.

2.2. Safety parameters

Two sets of quantities obtainable via experiments can be used for an intrinsically safe design of storage vessels and reactors containing HA/water/salt solutions: the onset and the maximum temperatures and pressures. These quantities can be retrieved from data acquired during any test run. For the sake of clarity, a generic plot of the results obtainable during a test is reported in Fig. 4.

More specifically, T_{onset} is intended as the minimum temperature at which the temperature profile deviates from the background heating rate due to an exothermic or endothermic process. Knowing the T_{onset} value, it is also possible to determine the time at which the measured temperature is equal to the onset one (t_{onset}) and the related pressure (P_{onset}). Whereas T_{max} is intended as the maximum measured temperature corresponding to an exothermic peak related to decomposition. Based on this temperature value, it is possible to determine the related time t_{max} and pressure P_{max}. The variables t_{onset} and t_{max} are used in Section 2.3. and 2.4. respectively to determine thermodynamic parameters useful for an intrinsic safety equipment design [42] and for constructing the stability diagram. Instead, T_{onset} can be used to determine process conditions because for reaction temperature greater than the onset, one decomposition occurs, and the system pressure starts to increase rapidly above P_{onset} causing the equipment explosion. Reducing T_{onset} determined via TS^u analysis by 75 °C, it is possible to quantify operative temperature for industrial-scale applications [43]. Alternatively, on the one hand, T_{max} can be used to ensure the mechanical integrity of the equipment in the worst-case thermal scenario and, on the other hand, P_{max} [44] and $(dP/dt)_{max}$ [33] are the main parameters to

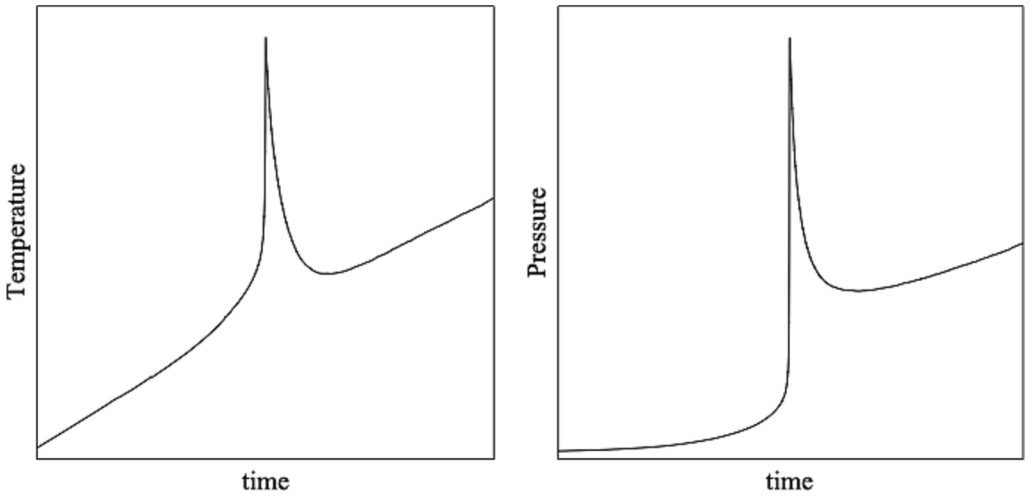

Fig. 4. Generic representation of data acquired during a test run: sample temperature and pressure.

consider during safety-relief valve design to avoid mechanical failure of reactors and storage vessels [45].

2.3. Data analysis

The values of T_{onset} were determined according to the method proposed by McIntosh and Waldram (2003) [46] based on the second time derivative of the measured temperature. T_{max} and P_{max} were assessed considering the maximum temperature and pressure measured during exothermic peaks. Once the t_{onset} and t_{max} values are collected, the enthalpy $\Delta\widetilde{H}_d\Big|_{T_{onset}}$ is calculated using the expression reported in Eq. (10) [47]. It is worth noting that $\Delta\widetilde{H}_{vap}$ is needed to disregard the contribution of the evaporation of the solvent (i.e., water) within the estimates of $\Delta\widetilde{H}_d\Big|_{T_{onset}}$. Eventually, in Eqs. (11) and (12), the expressions for the correction factor accounting for the non-perfect adiabaticity as a function of temperature $\Phi_{(T)}$, the adiabatic temperature rise during the reaction ΔT_{ad} and the time-averaged molar heat capacity between onset and decomposition temperature $\widetilde{C}_{p,sample}$ are reported, respectively.

$$\Delta\widetilde{H}_d = -\Delta\widetilde{H}_{vap} - \int_{t_{max}}^{t_{onset}} \Phi_{(T)}\widetilde{C}_{p,sample(T)}\left[\left(\frac{dT}{dt}\right)_{measured} - \left(\frac{dT}{dt}\right)_{baseline}\right]dt \tag{10}$$

$$\Phi = 1 + \frac{m_{cell}\widehat{C}_{p,cell}(T)}{m_{sample}\widehat{C}_{p,sample(T)}} \tag{11}$$

$$\Delta T_{ad} = \frac{-\Delta\widetilde{H}_d}{\widetilde{C}_{p,sample}\Big|_{\frac{T_{onset}+T_{max}}{2}}} \tag{12}$$

This work adopted two different strategies to quantify the above-reported heat capacities. $\widehat{C}_{p,cell(T)}$ is determined using the correlation reported in Eq. (13) [48]. Whereas, for $\widetilde{C}_{p,sample(T)}$ the method is based on a modified version of the relationship reported by Thomsen et al. (1996) [49] and Kumar and Patwardhans (1992) [50]. The modification aims to include the possibility of having multiple electrolytes in the considered aqueous mixture and to improve the accuracy of reproducing the experimental heat capacity of an aqueous solution reported in the literature [51,52]. The model equations are reported in Eqs. (14), (15) and (16), although the activity coefficients have been quantified using Pitzer's correlations [53].

$$\widehat{C}_{p,cell(T)} = 0.1026 + 4.4010^{-5}T + 1.3810^{-17}T^5 \tag{13}$$

$$\widetilde{C}_{p,s(T)} = \left(x_{solvent}|_1\widetilde{C}^0_{p,solvent} + \sum_i x_i|_1\overline{\widetilde{C}^0_{p,i}}\right) + \sum_i x_i|_1\left(\sum_j x_{j,i}\big|_2 J_{j,i(T)}\,\big|_2\right) \tag{14}$$

$$J_{j,i(298K)}\,\big|_2 = -2R_g298\left(\frac{\partial\ln\gamma^{\pm}_{j,i}\big|_2}{\partial T}\right)_{P,x}\Bigg|_{298K} - R_g298^2\left(\frac{\partial^2\ln\gamma^{\pm}_{j,i}\big|_2}{\partial T^2}\right)_{P,x}\Bigg|_{298K} \tag{15}$$

$$J_{j,i(T)}\,\big|_2 = J_{j,i(298K)}\,\big|_2 + J_{j,i(298K)}\,\big|_2 - \left[-2R_gT\left(\frac{\partial\ln\gamma^{\pm}_{j,i}\big|_2}{\partial T}\right)_{P,x} - R_gT^2\left(\frac{\partial^2\ln\gamma^{\pm}_{j,i}\big|_2}{\partial T^2}\right)_{P,x}\right] \tag{16}$$

Moving to the overall reaction kinetic data, coefficients were calculated according to the methodology proposed by Towsend and Tou (1980) [54]. More specifically, an iterative procedure is implemented assuming a given reaction order n and solving the set of Eqs. (17) and (18). Indeed, the apparent kinetic coefficient k_k were determined using the expression reported in Eq. (17), whereas the activation energy can be inferred by Eq. (18). Hence, reporting the trend for $\ln k_k$ against T^{-1} a linear profile is typically produced, having a slope of $-E_a/R_g$ and intercept of $\ln k_{k\infty}$. In the case of a non-linear trend, the value of the apparent reaction order n must be changed to obtain a linear relationship. Eventually, since the decomposition reaction occurs in the liquid phase, the effect of pressure on the reaction kinetic modelling has been neglected.

$$k_k = \frac{\left(\frac{dT}{dt}\right)_{measured} - \left(\frac{dT}{dt}\right)_{baseline}}{\Delta T_{ad}\left(\frac{T_{max}-T}{\Delta T_{ad}}\right)^n C_{A0}^{n-1}} \tag{17}$$

$$\ln k_k = -\frac{E_a}{R_g}\frac{1}{T} + \ln k_{k\infty} \tag{18}$$

2.4. Stability diagrams

A $Da-B$ diagram is produced, reporting the Damköhler number at which the system temperature reaches the onset value as a function of the dimensionless heat of the reaction B. Besides, an alternative criterion

Table 1
Safety, thermodynamic and kinetic parameters for the solutions containing HA in 10 %w.

%w HA		%w salt	T_{onset} [°C]	T_{max} [°C]	P_{max} [bar]	$\Delta\widetilde{H}_d$ [kJ/mol]	E_a [kJ/mol]
10	No salt		140 ± 9	195 ± 12	21 ± 3	−44.3 ± 0.1	126 ± 13
	HAS	1	134 ± 5	167 ± 3	8 ± 1	–	–
		2	112 ± 6	147 ± 5	5 ± 1	–	–
		10	129 ± 1	172 ± 1	10 ± 1	–	–
		20	122 ± 1	169 ± 10	9 ± 2	–	–
		30	119 ± 2	163 ± 12	8 ± 2	–	–
	HH	1	134 ± 7	157 ± 8	6 ± 1	–	–
		2	120 ± 6	155 ± 8	6 ± 1	–	–
		10	123 ± 1	163 ± 3	8 ± 1	–	–
		20	121 ± 5	157 ± 13	8 ± 2	–	–
		30	116 ± 2	152 ± 11	7 ± 1	–	–

Table 2
Safety, thermodynamic and kinetic parameters for solutions containing HA in 30 %w and 50 %w.

%w HA		%w salt	T_{onset} [°C]	T_{max} [°C]	P_{max} [bar]	$\Delta\widetilde{H}_d$ [kJ/mol]	E_a [kJ/mol]
30	No salt		132 ± 9	244 ± 1	46 ± 2	−69.6 ± 2.5	105 ± 8
	HAS	1	128 ± 7	185 ± 6	18 ± 1	−49.9 ± 1.2	165 ± 18
		2	104 ± 9	166 ± 8	15 ± 1	−51.1 ± 1.8	106 ± 10
		10	124 ± 1	229 ± 7	33 ± 3	−67.4 ± 1.1	124 ± 5
		20	111 ± 5	264 ± 4	58 ± 3	−101 ± 1	97.9 ± 9.1
		30	120 ± 2	243 ± 4	39 ± 2	−79.5 ± 0.3	108 ± 3
	HH	1	127 ± 11	176 ± 9	21 ± 6	−48.9 ± 2.7	139 ± 2
		2	119 ± 1	185 ± 9	19 ± 2	−52.2 ± 0.4	147 ± 2
		10	126 ± 5	228 ± 10	33 ± 4	−64.1 ± 2.3	114 ± 12
		20	125 ± 7	246 ± 5	39 ± 2	−76.3 ± 1.0	115 ± 1
		30	123 ± 1	244 ± 9	43 ± 2	−77.3 ± 1.6	108 ± 4
50	No salt		120 ± 8	238 ± 12	44 ± 7	−79.8 ± 0.2	103 ± 8
	HAS	1	119 ± 5	255 ± 9	51 ± 10	−96.5 ± 1.3	100 ± 4
		2	108 ± 5	253 ± 13	55 ± 3	−97.2 ± 5	85.8 ± 4
		10	112 ± 5	261 ± 5	58 ± 4	−98.2 ± 3.3	98.7 ± 14.0
		20	111 ± 5	264 ± 4	58 ± 3	−101 ± 1	97.9 ± 9.1
		30	108 ± 5	270 ± 6	59 ± 3	−109 ± 1	92.6 ± 9.6
	HH	1	119 ± 2	241 ± 6	48 ± 3	−78.1 ± 0.9	117 ± 6
		2	117 ± 2	250 ± 3	55 ± 3	−82.1 ± 0.2	111 ± 7
		10	113 ± 7	269 ± 4	61 ± 5	−90.3 ± 0.8	103 ± 9
		20	110 ± 8	276 ± 5	66 ± 8	−97.7 ± 8.4	96.2 ± 10.4
		30	108 ± 3	287 ± 5	64 ± 3	−107 ± 1	87.8 ± 8.7

was implemented to check the reliability of the method, i.e., $dT/dt = 0$, following a prevalent approach in the current literature [55]. In this way, it is possible to determine the batch time t guarantee the absence of runaway for a specific set of process conditions (i.e., T_0 and C_{A0}) and reaction characteristics (i.e., E_a, n, $\Delta\widetilde{H}_d$ and T_{onset}). Even if this type of diagram is commonly used in continuous reactors to relate the reactivity and the exothermicity of the reactive system, it can also be employed for adiabatic batch systems if a driving criterion for selecting Da is provided. Because the Damköhler number is not a system-independent parameter but is the dimensionless dependent variable of the constitutive physicochemical model, the need for the selection criteria for Da arises. In this way, the effect of the variation of C_{A0} and T_0 can be directly considered, performing simulations for different values of these two input parameters. Eventually, the definitions of Da and B, related to the stability diagram, are reported in Eqs. (19) and (20).

$$Da = tk_k|_{T_0} C_{A0}^{n-1} \tag{19}$$

$$B = \frac{\left(-\Delta\widetilde{H}_d\right) C_{A0}}{\rho \widetilde{C}_p T_0} \gamma \tag{20}$$

3. Results and discussions

The kinetic and thermodynamic properties of the different HA/water/salt solutions were determined according to the methodology reported in Section 2 and compared with HA/water solutions. The physicochemical properties were determined using TS^U analysis to assess the safety parameters and construct system stability diagrams. The results of the experimental campaign are summarized in Tables 1 and 2, containing the data for water solutions of HA respectively in 10 %w, 30 %w, and 50 %w. Specifically, each quantity reported is the mean value obtained with the 2 °C min^{-1} and 5 °C min^{-1} heating rates to have a general representation of the thermal decomposition phenomenon, less dependent than possible from the experiments set up. For the sake of clarity, the discussion of the presented results is separated to highlight the effects of a single variable per time, at first.

3.1. Effect of hydroxylamine content

Quite clearly, the behaviour of the mixtures significantly depends on the HA concentration. Indeed, T_{onset} decreases and $\Delta\widetilde{H}_d$ increases as the amount of HA contained in the samples increases. This applies to samples prepared with the same amount of generic salt. Thus, the decomposition becomes respectively more susceptible and more exothermic. A peculiar behaviour can be observed for the 10 %w HA solutions. The HA/water mixture exhibits an exothermic decomposition without adding HAS or HH, but no runaway phenomena are detected. A low $\Delta\widetilde{H}_d$ is associated with thermal degradation, with a weak temperature increment from the onset to the maximum value. Thus, a marked peak in the temperature and pressure profiles cannot be observed.

3.2. Effect of salt addition

Regarding the amount of salt added to the HA/water solutions, this parameter mainly affects the T_{max}, P_{max} and E_a values and slightly perturbates the T_{onset} and the $\Delta\widetilde{H}_d$. Singular behaviour is the one revealed for the 10 %w HA solutions. Once a generic salt is added, a feeble decomposition reaction can be detected, with shallow thermal and mechanical associated effects. This inhibition of the decomposition features depends on the amount of salt added; more significant inhibitions are associated with lower added salt amounts. Quite clearly, this contributes to stabilising the considered aqueous solution. For clarity, it is better to underline that salt addition can stabilise the mixture, increasing the activation energy and the onset temperature, and decreasing the decomposition enthalpy and the maximum temperature and pressure. Indeed, as the activation energy increases, the energy barrier that must be overcome to trigger the decomposition increases. Increasing the onset temperature, the amount of thermal energy the mixture must have before the thermal degradation takes place must be higher. A lower reaction enthalpy means that the mix generates less thermal energy due to its degradation, lowering the severity of the associated thermal runaway. Eventually, lower maximum temperature and pressures reached during the thermal degradation are indexes of a lower side effect of the decomposition itself.

Regardless of the HA concentration, the effect of the added amount of salt can be distinguished for diluted (i.e., from 1 %w to 2 %w) and concentrated (i.e., from 10 %w to 50 %w) samples. A more general behaviour can be observed for the concentrated solutions independent of the salt added. Increasing the salt amount makes the solution more susceptible to decomposition, and the related thermal and mechanical phenomena seem more violent. It is worth noting a general reduction in the T_{onset} and E_a with higher amounts of added salts, confirming the higher tendency of the mixture to decompose and, on the other hand, also a general augmentation in the T_{max}, P_{max} and $\Delta\widetilde{H}_d$, validating the observation of higher hazards related to the decomposition reaction.

Focusing on the diluted mixtures, the reduction in the onset temperature is more pronounced in the presence of a higher initial %w of HA, taking as a reference value the one reported for HA/water solution with the same initial %w of HA. As can be noted from Tables 1 and 2, the reported T_{onset} for solutions with 2 %w of HAS or HH is lower than the T_{onset} for 1 %w of HAS or HH, for each value of %w of HA analysed. This deviation from the HA/water reference value destabilizes the reacting mixtures, anticipating the temperature at which exothermic decompositions occur. Also, the T_{max} and P_{max} values deviate in diluted solutions after salt addition. However, moving from 50 %w to 30 %w and 10 %w of HA, the maximum temperature and pressure values first increase from the HA/water reference solution and then decrease. This evidence can be considered a stabilizing effect for the 30 %w and 10 %w HA solutions and a destabilizing one for the 50 %w of HA. The same feature is observed for the $\Delta\widetilde{H}_d$ (the 50 %w HA solution has a greater $\Delta\widetilde{H}_d$ compared to the pure HA/water solution and is lower in the 30 %w HA solution) but is slightly greater in the 2 %w than in the 1 %w, contrary to the T_{onset}, T_{max} and P_{max} trend. Recalling that lower $\Delta\widetilde{H}_d$ means lower exothermic decompositions, adding a low amount of salt to a 50 %w HA/water solution has a destabilizing effect, whereas, in a 30 %w HA/water solution, it contributed to reducing the thermal hazards. Eventually, also for the E_a moving from 50 %w to 30 %w HA/water solutions, the lower content of HA-derived salts first enhances the probability of decomposition, reducing the activation energy values, but then it hinders the thermal degradation, increasing the E_a value. Mixtures with 2 %w of added HAS are more prone to decomposition than 1 %w because of a generally lower value in the activation energy, independently of the initial content of HA in water. However, the opposite trend is observed in the case of the HH salt, confirming a dependency on the type of added salt on the decomposition observed pathway. For the sake of clarity, in Fig. 5, the experimental temperature and pressure decomposition profiles for 50 %w HA solution with all the examined %w of HAS under a heating rate of 2 °C min^{-1} have been reported. The same plot obtained with HH is reported in the Supplementary Material.

3.3. Double peak behaviour

A double peak behaviour associated with thermal decomposition can be observed for the 10 %w HA water solutions containing HAS or HH salts. As can be seen in Table 3, two values of onset and maximum temperatures were detected. This behaviour can be explained by recalling that HA, HAS, or HH are present in the water solution. A possible explanation is that the first peak is associated with HA decomposition, whereas the second refers to salt decomposition. According to Gigante et al. (2004) and Cisneros et al. (2003), the HA decomposition temperature is lower than the HAS or HH one,

Table 3
Double-peak values for the 10 %w HA water solution with HAS and HH.

%w HA	%w salt	T_{onset} [°C]		T_{max} [°C]	
10	HAS − 20	122 ± 1	176 ± 11	169 ± 10	188 ± 13
	HAS − 30	119 ± 2	181 ± 7	163 ± 12	188 ± 5
	HH − 20	121 ± 5	172 ± 15	157 ± 13	188 ± 10
	HH − 30	116 ± 2	157 ± 12	152 ± 11	180 ± 6

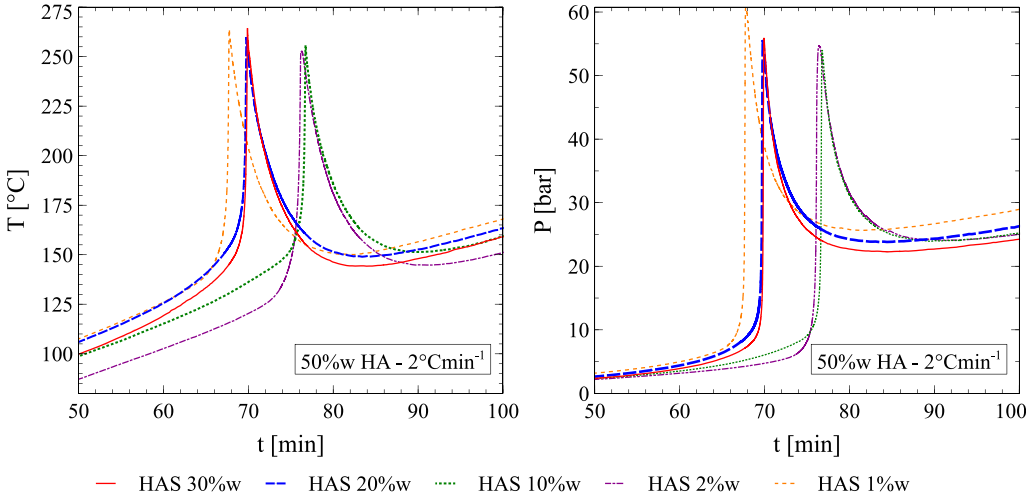

Fig. 5. Experimental temperature and pressure decomposition peaks for 50 %w HA solutions with all the examined %w of HAS under a heating rate of 2 °C min^{-1}.

confirming the previous statement. Moreover, it can be considered that due to the low amount of HA dissolved (i.e., 10 %w), the first decomposition cannot cover the entire range of temperature from HA to HAS or HH decay. Thus, the salt thermal degradation starts to be detectable, and the second peak is observable. However, with 10 %w salts or less, the second peak is no longer noticeable because of the too-low quantity of reactant contained in the mixture.

3.4. Stability diagram

Based on the experimental data reported in Tables 1 and 2, the solutions with 50 %w HA and 30 %w HH can be considered the most critical because they exhibit the lowest T_{onset} and E_a and the highest T_{max}, P_{max} and $\Delta\widetilde{H}_d$. Thus, this kind of mixture was selected as the representative case for the analysis of system stability diagrams, being the worst-case scenario among the screened ones. Eventually, all the considerations drawn for the representative case proposed can be extended to other scenarios.

First, the applicability of VMWT in the construction of stability diagrams has been verified. As expected, the theory has not produced credible results from a numerical or a physicochemical point of view. Indeed, a change in the Da span for the simulations can modify the B_{crit}, highlighting an essential numerical instability of the method in which the outcome is sensitive to the simulations' boundary conditions. This is explained by considering that, for low values of B, with sufficiently high Da, the system exhibits fully developed temperature profiles. Moreover, for slight perturbation of the input parameters, the severity of the temperature development can result in runaway conditions for practically every B. In addition, the profile $S(\theta^*;B)$ is characterized by multiple maximums for different values of B. Furthermore, the magnitude of the maximum increases with B, making the determination of B_{crit} unsuccessful. From a physicochemical perspective, this behaviour is expected because the system's sensibility is likely to increase as the severity of the exothermic reaction increases. For these reasons, the employment of different runaway criteria has been validated, and the outcomes of the proposed strategies have been reported subsequently.

As can be noticed in [27], the Da, γ and B numbers depend on T_0. Thus, the $Da-B$ diagram can be built by selecting a value of the initial reaction temperature, and the t value determined is dependent on this choice. Fig. 6 represents the stability diagram for $T_0 = 300K$ and all the other parameters (i.e., C_{A0}, E_a, $\Delta\widetilde{H}_r$, ρ, $\widehat{C}_p$, $k_{k\infty}$ and T_{onset}) are related to the solution with 50 %w HA and 30 %w HH. For the sake of clarity, only one initial temperature outcome has been reported in the $Da-B$ diagram, but in the following the effect of T_0 on t is further discussed.

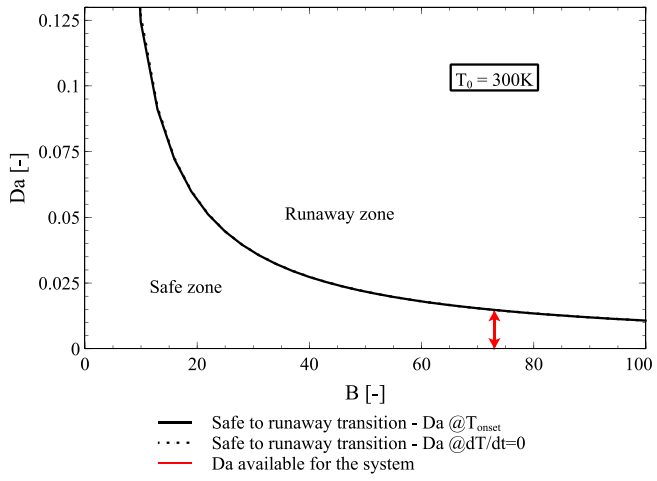

Fig. 6. Da-B diagram for the sample 50 %w HA and 30 %w HH based on the data collected having an initial temperature of 300 K.

Table 4
Batch time t of the solution 50 %w of HA and 30 %w of HH at different initial temperatures T_0 calculated according to the two approaches for determining Da.

	t [min]	
T_0 [K]	$Da\|_{T_{onset}}$	$Da\|_{dT/dt=0}$
300	7994	8005
325	623	632
350	64	73

Both the adopted criteria for determining Da (i.e., the one proposed by Strozzi et al. (1999) and the one presented in this work) produced the same safe-runaway transition curve. However, considering T_{onset} instead of $dT/dt = 0$, a more stringent and conservative safe zone can be determined. The effect of using a criterion preferentially has been quantified and reported in Table 4 for various T_0. A variation in the initial reaction temperature has not only the effect of reducing B but also affects $k_k|_{T_0}$, which is in the definition of Da. Because of Da depends exponentially on T_0, and B depends only quadratically on the initial reaction temperature; the final reduction in the batch time t is evident even for a slight variation of the input parameter. Consequently, a decrease of a few degrees in the initial reaction temperature has a relevant impact on the system safety, requiring longer time at adiabatic conditions before runaway conditions are achieved. Thus, low-temperature processes must be preferred, giving the operators more time to restore control of reactive systems in the case of undesired scenarios.

Starting from the stability diagram of Fig. 4, it is possible to establish intrinsically safe operations to prevent the runaway phenomenon. Indeed, at $T_0 = 300K$, and for $B < 10$ approximately, the safe-transition curve no longer exists. Thus, there is no value of t able to trigger a runaway phenomenon. To establish these intrinsic safe conditions, considering $T_0 = 300K$, the B number must be reduced from the process condition examined (i.e., B equals 72.95) to acting, for example, on C_{A0} Also, the effect of the initial concentration of the main reactant on the apparent decomposition dynamic in terms of kinetic, thermodynamic, and onset features is considered.

3.5. General guidelines for inherently safe operations

Pseudo-adiabatic conditions in the process industry can be established accidentally. Suppose the fluid is prone to decomposition like an aqueous mixture of HA or HA/water/salt solution, hazardous conditions for the process plat could be triggered. Indeed, pumps and impellers could not work, and if draining valves are not properly designed (i.e., fail open) or fail to operate, pipelines and equipment must be emptied manually. Using information obtained through stability diagrams (i.e., the adiabatic batch time before runaway as a function of the initial reaction temperature and main reactant concentration) makes it possible to quantify the time available for securing the productive equipment. Moreover, if the available adiabatic batch time is reasonably long, like in the case of $T_0 = 300K$ (Table 4), it is possible to prioritize other corrective actions during accidental scenarios.

In the design phase, the stability diagram provides crucial directions for selecting a proper safe operating temperature. Considering a productive route to synthesize a compound prone to exothermic thermal degradation, the first step will be a calorimetric analysis. Then, the acquired kinetic, thermodynamic and onset information can be used for design purposes. To be more specific, a reactor operation diagram can be built considering the reactor configuration used (i.e., CSTR, PFR, series of CSTRs, fixed bed, etc.) and increasingly detailed kinetic schemes with reactions in series and/or parallel. Since an operating temperature has not been selected, it could be a degree of freedom with the reactor size and geometry. Before doing a detailed analysis, a preliminary screening can be performed based on the decomposition pathway, finding a

reference T_0 value aimed to limit the undesired chemical reaction. Indeed, the stability diagram proposed in this work is general and independent of any reactor configuration. Then, it is possible to perform more detailed evaluations, refining the conclusions drawn.

Concerning QRA, information acquired through the stability diagram can be used to quantify the runaway reaction probability. Following the work developed by Juncheng et al. (2020) [56], the time needed in adiabatic conditions to reach the onset temperature can be used as a more conservative criterion than the TMR_{ad}. Because a detailed methodology for a QRA of runaway reaction has not been established yet, developing new standards for a safety evaluation is fundamental for new or existing processes that involve thermally unstable compounds subjected to chemical or physical transformations.

4. Conclusions

When molecules prone to decomposition, like hydroxylamine, are processed, thermal analysis is paramount to enhance process safety. To this aim, the decomposition kinetic, thermodynamic, and onset features must be quantitatively assessed to avoid significant accident scenarios for industrial-scale operations. To reduce the occurrence of thermal instability scenarios, the present work deals with the effect of hydroxylamine-derived salt as a mitigating agent. Moreover, the acquired information has also been involved in determining stability diagrams to outline the inherently safe zone with respect to runaway conditions and practical precautions to avoid hazardous operations. Eventually, the proposed methodology could be generalized and applied to other molecules as a structured analysis tool.

The results show that the extent of the decomposition inhibition depends on the type and amount of hydroxylamine-derived salt added to a hydroxylamine/water solution. The reason behind this attenuation can be found in a modification of the overall reaction dynamic, as shown by the double peak behaviour detected. However, a general quantitative description of the effect of the type and amount of salt added on the decomposition inhibition cannot be drawn, and a specific evaluation is required on a case-by-case scenario. According to the results, increasing the salt amount makes the aqueous solutions of HA more susceptible to decomposition with a lower onset temperature and apparent activation energy, resulting in more severe outcomes. On the contrary, diluted quantities of salts, under specific conditions, have a stabilizing effect on the aqueous solutions of HA. An inherently safe zone for operating systems with HA in water and salts is achieved for $B < 10$ at an initial temperature of 300 K.

CRediT authorship contribution statement

Giuseppe Andriani: Conceptualization, Formal analysis, Investigation, Methodology, Writing – original draft, Data curation. **Gianmaria Pio:** Methodology, Validation, Writing – review & editing. **Chiara Vianello:** Funding acquisition, Project administration, Resources, Writing – review & editing. **Paolo Mocellin:** Conceptualization, Funding acquisition, Investigation, Project administration, Supervision, Writing – original draft, Writing – review & editing. **Ernesto Salzano:** Project administration, Resources, Supervision, Writing – review & editing.

Declaration of competing interest

The authors declare that they have no known competing financial interests or personal relationships that could have appeared to influence the work reported in this paper.

Data availability

Data will be made available on request.

Appendix A. Supplementary data

Supplementary data to this article can be found online at https://doi.org/10.1016/j.cej.2024.148894.

References

[1] J. Clayden, N. Greeves, S. Warren, Organic Chemistry, 2nd ed., Oxford University Press, 2012.
[2] M.M.M. Kuypers, H.K. Marchant, B. Kartal, The microbial nitrogen-cycling network, Nat. Rev.Microbiol 16 (5) (May 2018) 263–276, https://doi.org/10.1038/nrmicro.2018.9.
[3] P. Gross, R.P. Smith, Biologic Activity of Hydroxylamine: A Review, Crit Rev Toxicol 14 (1) (1985) 87–99, https://doi.org/10.3109/10408448509023765.
[4] Ullmann's Encyclopedia of Industrial Chemistry, 7th ed, Wiley-VCH, 2011.
[5] Q. Wang, C. Wei, L.M. Pérez, W.J. Rogers, M.B. Hall, M.S. Mannan, Thermal decomposition pathways of hydroxylamine: Theoretical investigation on the initial steps, J. Phys. Chem. A 114 (34) (Sep. 2010) 9262–9269, https://doi.org/10.1021/jp104144x.
[6] K. Krishna, et al., Hydroxylamine production: Will a QRA help you decide? Reliab Eng Syst Saf 81 (2) (2003) 215–224, https://doi.org/10.1016/S0951-8320(03)00115-7.
[7] Y. Lwata, H. Koseki, Risk Evaluation of Decomposition of Hydrosylamine/Water Solution at Various Concentrations, Process Saf. Prog. 21 (2) (2002) 136–141, https://doi.org/10.1002/prs.680210210.
[8] T. Adamopoulou, et al., Thermal decomposition of hydroxylamine: Isoperibolic calorimetric measurements at different conditions, J. Hazard. Mater. 254–255 (1) (Jun. 2013) 382–389, https://doi.org/10.1016/j.jhazmat.2013.03.031.
[9] J. Zheng, et al., Thermal decomposition behavior, thermal stability and thermal explosion risk evaluation of a novel green hydroxylamine ionic liquid salt, J Mol Liq 348 (Feb. 2022), https://doi.org/10.1016/j.molliq.2021.118407.
[10] L.O. Cisneros, W.J. Rogers, M.S. Mannan, Adiabatic calorimetric decomposition studies of 50 wt.% hydroxylamine/water, J. Hazard. Mater. 82 (1) (2001) 13–24, https://doi.org/10.1016/s0304-3894(00)00356-3.
[11] Y. Iwata, H. Koseki, F. Hosoya, Study on decomposition of hydroxylamine/water solution, J Loss Prev Process Ind 16 (1) (2003) 41–53, https://doi.org/10.1016/S0950-4230(02)00072-4.
[12] L.A. Long, The explosion at concept sciences: Hazards of hydroxylamine, Process Saf. Prog. 23 (2) (Jun. 2004) 114–120, https://doi.org/10.1002/prs.10013.
[13] "ARIA database." [Online]. Available: https://www.aria.developpement-durable.gouv.fr/the-barpi/the-aria-database/?lang=en.
[14] "FACTS database." [Online]. Available: http://www.factsonline.nl/browse-chemical-accidents-in-database.
[15] C. Wei, S.R. Saraf, W.J. Rogers, M. Sam Mannan, Thermal runaway reaction hazards and mechanisms of hydroxylamine with acid/base contaminants, Thermochim Acta 421 (1–2) (Nov. 2004) 1–9, https://doi.org/10.1016/j.tca.2004.02.012.
[16] E. Danzi, L. Malmo, G. Pio, and E. Salzano, "Thermal stability of chemicals under fire conditions: the case of hydroxylamine sulphate," 2019. [Online]. Available: http://www.icders.org/ICDERS2019/abstracts/ICDERS2019-130.pdf.
[17] L.O. Cisneros, W.J. Rogers, M. Mannan, Effect of air in the thermal decomposition of 50 mass% hydroxylamine/water, J. Hazard. Mater. 95 (2002) 13–25, https://doi.org/10.1016/s0304-3894(02)00163-2.
[18] L.O. Cisneros, X. Wu, W.J. Rogers, M.S. Mannan, J. Park, S.W. North, Decomposition products of 50 mass% hydroxylamine/water under runaway reaction conditions, Process Saf Environ Prot 81 (2) (2003) 121–124, https://doi.org/10.1205/095758203321832598.
[19] L. Gigante *et al.*, "Hydroxylamine and its salts: thermoanalytical and safety study," *Rivista dei Combustibili*, vol. 58, no. 4, pp. 137–152, 2004, [Online]. Available: https://inis.iaea.org/search/search.aspx?orig_q=RN:36106099.
[20] L. Shao, et al., Hydroxylamine hydrochloride: A novel anode material for high capacity lithium-ion batteries, J. Power Sources 272 (Dec. 2014) 39–44, https://doi.org/10.1016/j.jpowsour.2014.08.065.
[21] L.O. Cisneros, W.J. Rogers, M.S. Mannan, Comparison of the thermal decomposition behavior for members of the hydroxylamine family, Thermochim Acta 414 (2) (May 2004) 177–183, https://doi.org/10.1016/j.tca.2003.09.023.
[22] D.G. Harlow, S.B. Agnew, W. Hanford Company, G. Scott Barney Westinghouse Savannah River Company, J. Malvyn McKibben Parallax, and r. Garber, "technical Report on Hydroxylamine Nitrate" (1998).
[23] J. Liu, Z. An, Q. Zhang, C. Wang, Thermal decomposition of hydroxylamine nitrate studied by differential scanning calorimetry analysis and density functional theory calculations, Prog. React. Kinet. Mech. 42 (4) (2017) 334–343, https://doi.org/10.3184/146867817X14954764850351.
[24] L.O. Cisneros, W.J. Rogers, M.S. Mannan, Adiabatic calorimetric decomposition studies of 35 mass% hydroxylamine hydrochloride/water, Can. J. Chem. Eng. 82 (6) (2004) 1307–1312, https://doi.org/10.1002/cjce.5450820620.
[25] M. Kumasaki, Calorimetric study on the decomposition of hydroxylamine in the presence of transition metals, J Hazard Mater, vol. 115, no. 1-3 SPEC. ISS., pp. 57–62, Nov. 2004, doi: 10.1016/j.jhazmat.2004.06.020.
[26] L.O. Cisneros, W.J. Rogers, M.S. Mannan, X. Li, H. Koseki, Effect of iron ion in the thermal decomposition of 50 mass % hydroxylamine/water solutions, J Chem Eng Data 48 (5) (Sep. 2003) 1164–1169, https://doi.org/10.1021/je030121p.

[27] J. Jiang, J. Jiang, Y. Pan, R. Wang, P. Tang, Investigation on thermal runaway in batch reactors by parametric sensitivity analysis, Chem. Eng Technol 34 (9) (Sep. 2011) 1521–1528, https://doi.org/10.1002/ceat.201000517.
[28] A. Varma, M. Morbidelli, H. Wu, Parametric Sensitivity in Chemical Systems, 1st ed., Cambridge University Press, 1999.
[29] K.R. Westerterp, E.J. Molga, Safety and runaway prevention in batch and semibatch reactors - A review, Chem. Eng. Res. Des. 84 (7A) (2006) 543–552, https://doi.org/10.1205/cherd.05221.
[30] G. Andriani, B.A. De Liso, G. Pio, E. Salzano, Design of sustainable reactor based on key performance indicators, Chem. Eng Sci 285 (Mar. 2024) 119591, https://doi.org/10.1016/j.ces.2023.119591.
[31] T. Ozawa, Thermal analysis - review and prospect, Thermochim Acta 355 (1–2) (2000) 35–42, https://doi.org/10.1016/S0040-6031(00)00435-4.
[32] S. Vyazovkin, N. Koga, and C. Schick, Handbook of Thermal Analysis and Calorimetry: Recent Advances, Techniques and Applications, 2nd ed., vol. 6. Elsevier, 2018.
[33] C.H. Spink, Differential Scanning Calorimetry, Methods Cell Biol. 84 (2008) 115–141, https://doi.org/10.1016/S0091-679X(07)84005-2.
[34] N. Saadatkhah et al., "Experimental methods in chemical engineering: Thermogravimetric analysis—TGA," Canadian Journal of Chemical Engineering, vol. 98, no. 1. Wiley-Liss Inc., pp. 34–43, Jan. 01, 2020. doi: 10.1002/cjce.23673.
[35] M. A. A. O'Neill and S. Gaisford, "Application and use of isothermal calorimetry in pharmaceutical development," International Journal of Pharmaceutics, vol. 417, no. 1–2. Elsevier B.V., pp. 83–93, Sep. 30, 2011. doi: 10.1016/j.ijpharm.2011.01.038.
[36] R.N. Landau, Expanding the role of reaction calorimetry, Thermochim Acta 289 (1996) 101–126, https://doi.org/10.1016/S0040-6031(96)03081-X.
[37] R.S. Jessup, Precise Measurement of Heat of Combustion With a Bomb Calorimeter, 1st ed., U.S. Department of Commerce - National Bureau of Standards, 1960.
[38] M. N. Richard and J. R. Dahn, "Part I: Accelerating Rate Calorimetry Study on the Thermal Stability of Lithium Intercalated Graphite in Electrolyte I. Experimental," *J Electrochem Soc*, vol. 146, no. 6, 1999, doi: 10.1149/1.1391893.
[39] C. Vianello, E. Salzano, G. Maschio, Safety parameters and preliminary decomposition kinetic of organo-peroxy acids in aqueous phase, Chem. Eng Trans 43 (2015) 2371–2376, https://doi.org/10.3303/CET1543396.
[40] G. Pio, P. Mocellin, C. Vianello, E. Salzano, A detailed kinetic model for the thermal decomposition of hydroxylamine, J. Hazard. Mater. 416 (Aug. 2021), https://doi.org/10.1016/j.jhazmat.2021.125641.
[41] C. Vianello, E. Salzano, G. Maschio, Thermal behaviour of Peracetic Acid for the epoxydation of vegetable oils in the presence of catalyst, Process Saf. Environ. Prot. 116 (May 2018) 718–726, https://doi.org/10.1016/j.psep.2018.03.030.
[42] T. Kletz, P. Amyotte, Process Plants: A Handbook for Inherently Safer Design, 2nd ed., CRC Press - Taylor & Francis Group, 2010.
[43] A.D. Allian, N.P. Shah, A.C. Ferretti, D.B. Brown, S.P. Kolis, J.B. Sperry, Process safety in the pharmaceutical industry-part I: Thermal and reaction hazard evaluation processes and techniques, Org. Process Res. Dev. 24 (11) (Nov. 2020) 2529–2548, https://doi.org/10.1021/acs.oprd.0c00226.
[44] S. Veedhi, A. Sawant, Designing a safer process for the reaction of TFA with sodium borohydride in THF by calorimetric technique, J Therm Anal Calorim 111 (2) (Feb. 2013) 1093–1097, https://doi.org/10.1007/s10973-012-2514-0.
[45] D.A. Crowl and Louvar Joseph F., Chemical Process Safety Fundamentals with Applications, 3rd ed. 2011.
[46] R.D. Mcintosh, S.P. Waldram, Obtaining more, and better, information from simple ramped temperature screening tests, J Therm Anal Calorim 73 (1) (2003) 35–52, https://doi.org/10.1023/A:1025169121312.
[47] C. Vianello, E. Salzano, G. Maschio, Kinetics and safety analysis of peracetic acid, Chem. Eng Trans 48 (2016) 559–564, https://doi.org/10.3303/CET1648094.
[48] R.R. Thais, J.P. Kohn, Heat Capacity of Hastelloy Alloy X, J Chem Eng Data 9 (4) (1964) 546–547, https://doi.org/10.1021/je60023a024.
[49] K. Thomsen, P. Rasmussen, R. Gani, Correlation and prediction of thermal properties and phase behaviour for a class of aqueous electrolyte systems, Chem. Eng Sci 51 (14) (1996) 3675–3683, https://doi.org/10.1016/0009-2509(95)00418-1.
[50] A. Kumar, V.S. Patwardhans, Aqueous solutions of single electrolytes: thermodynamic properties at high temperature and concentration, Chem. Eng Sci 47 (15–16) (1992) 4039–4047, https://doi.org/10.1016/0009-2509(92)85154-4.
[51] M.C.F. Magalhães, E. Königsberger, P.M. May, G. Hefter, Heat capacities of concentrated aqueous solutions of sodium sulfate, sodium carbonate, and sodium hydroxide at 25 °C, J Chem Eng Data 47 (3) (May 2002) 590–598, https://doi.org/10.1021/je010314h.
[52] E. Königsberger, L.C. Königsberger, P. May, B. Harris, Properties of electrolyte solutions relevant to high concentration chloride leaching. II. Density, viscosity and heat capacity of mixed aqueous solutions of magnesium chloride and nickel chloride measured to 90 °C, Hydrometall. 90 (2–4) (Feb. 2008) 168–176, https://doi.org/10.1016/j.hydromet.2007.10.007.
[53] L.L. Lee, Molecular Thermodynamics of Electrolyte Solutions, 1st ed., World Scientific, 2008.
[54] D.I. Townsend, J.C. Tou, Thermal hazard evaluation by an accelerating rate calorimeter, Thermochim. Acta 37 (1) (1980) 1–30, https://doi.org/10.1016/0040-6031(80)85001-5.
[55] F. Strozzi, J.M.Z. Zaldıvaŕ, A.E. Kronberg, K.R. Westerterp, On-line runaway detection in batch reactors using chaos theory techniques, AIChE J. 45 (11) (1999) 2429–2443, https://doi.org/10.1002/aic.690451116.
[56] J. Juncheng, W. Dan, N. Lei, F. Gang, P. Yong, Inherent thermal runaway hazard evaluation method of chemical process based on fire and explosion index, J Loss Prev Process Ind 64 (Mar. 2020), https://doi.org/10.1016/j.jlp.2020.104093.